Design of ZnS antireflective microstructures for mid- and far-infrared applications

Y. J. Yoo, K. S. Chang, S. W. Hong & Y. M. Song

Optical and Quantum Electronics

ISSN 0306-8919

Opt Quant Electron
DOI 10.1007/s11082-015-0143-0

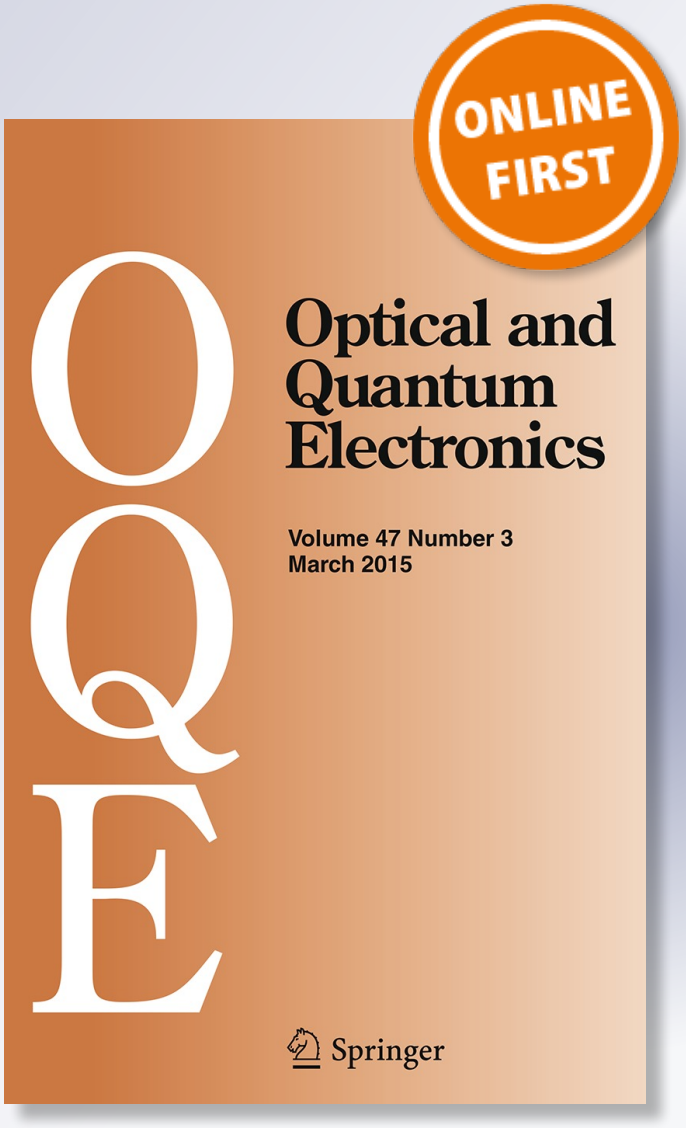

Springer

Opt Quant Electron
DOI 10.1007/s11082-015-0143-0

Design of ZnS antireflective microstructures for mid- and far-infrared applications

Y. J. Yoo · K. S. Chang · S. W. Hong · Y. M. Song

Received: 30 September 2014 / Accepted: 19 February 2015

Abstract We present broadband antireflective microstructures (AMSs) for high-performance imaging systems in mid- and far-infrared wavelength ranges. Diffraction efficiencies of AMSs on ZnS substrates were calculated using a rigorous coupled wave analysis method. The results show the effect of height, period, and shape of AMSs on the reflection characteristics. We also discuss the optimum geometry of AMSs by considering fabrication tolerances.

Keywords Subwavelength grating · Antireflection · Microstructure · Zinc sulfide

1 Introduction

Fresnel reflection due to refractive index mismatch at the interface between two different media can significantly deteriorate the performance of many optic components (lens, optical fibers, windows, etc.) and optoelectronic devices (solar cells, photodetectors, light emitting diodes, etc.). Conventional thin-film antireflection coatings (ARCs) exhibit reduced reflection by their interference principle, however, it can only works in a limited wavelength range. For mid-infrared (IR) or far-IR applications, this fact becomes a strong

Y. J. Yoo · Y. M. Song (✉)
Department of Electronics Engineering, Pusan National University, 2 Busandaehak-ro 63beon-gil, Geumjeong-gu, Busan 609-735, Republic of Korea
e-mail: ysong@pusan.ac.kr

K. S. Chang
Center for Analytical Instrumentation Development, Korea Basic Science Institute, 169-148 Gwahak-ro, Yuseong-gu, Daejeon 305-806, Republic of Korea

S. W. Hong (✉)
Department of Cogno-Mechatronics Engineering, Pusan National University, 2 Busandaehak-ro 63beon-gil, Geumjeong-gu, Busan 609-735, Republic of Korea
e-mail: swhong@pusan.ac.kr

Published online: 04 March 2015

obstacle. Most of the materials that are appropriate for infrared applications, such as germanium (Ge), zinc sulfide (ZnS), and zinc selenide (ZnSe), have much higher refractive indices than that of transparent glasses/polymers, which give rise to high Fresnel reflection losses. For broadband antireflection in the IR region, multilayer stacks with thickness of few micrometers are needed (Phillips et al. 2008; Ghosh and Bandyopadhyay 2005), which causes increased fabrication time and cost. Moreover, thin film technology has inherent problems such as adhesion, thermal mismatch, and the stability of the thin film stacks (Lalanne and Morris 1996).

As an alternative to thin film coatings, the studies on biomimetic subwavelength structures, originally inspired by the excellent antireflective capability of corneal of night active insects, have been developing rapidly. The basic idea is that the nanostructured coating-materials are capable of creating a gradient refractive index profile due to their tapered morphology, and consequently forms their unique broad wavelength antireflection property (Fig. 1). In recent years, various nanofabrication techniques and new antireflective materials have emerged (Kanamori et al. 1999; Yu et al. 2003; Striemer and Fauchet 2002; Song et al. 2010, 2011). Nevertheless, reported works mainly focus on the AR properties in the visible and near-IR wavelength ranges. It is known that the tapered structures with a taller height and a shorter period are desirable for broadband AR properties. From this point of view, nanotip arrays with a high aspect ratio (>20) are ideal, however, it causes complicated fabrication procedure. Hence, it is mandatory to determine an optimum geometry of AR structures within a reasonable aspect ratio. In this study, we have calculated the diffraction efficiency of the antireflective microstructures (AMSs) on ZnS substrates with different heights and periods. Optimum geometries are discussed in terms of reflectance and grating structures.

2 Simulation results and discussion

Figure 1b show schematic illustrations of AMSs on a silicon substrate. In this calculation, we used a crystalline ZnS substrate as an infrared window material. Because ZnS is transparent in the wavelength ranges of 0.4–12 μm, it is commonly used as a window materials for mid-IR (3–5 μm) and far-IR (8–14 μm) applications. In general, the 8–14 μm band is preferred for high performance thermal imaging because of it higher sensitivity to ambient temperature objects and its better transmission through mist and smoke. On the other hand, the 3–5 μm band may be more appropriate for hotter object, or if sensitivity is less important than contrast (Rogalski and Chrzanowski 2002). The theoretical calculations

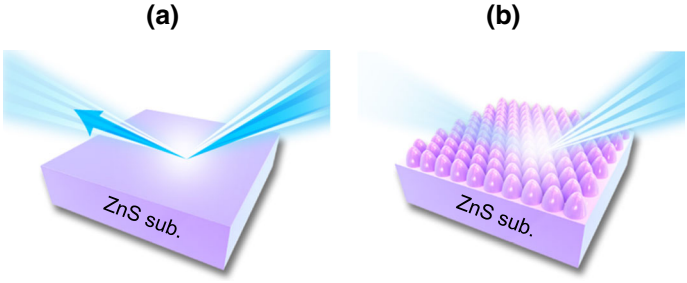

Fig. 1 Schematic illustrations of light reflection **a** at a flat surface and **b** at antireflective micro-structures (AMSs) on ZnS substrates

of reflectance were done by using a rigorous coupled wave analysis (RCWA) method (Moharam 1988) and materials dispersion was considered. To enhance the AR properties, parabola shape with a sixfold hexagonal symmetry, which provides linear graded refractive index profile, was used.

Figure 2 shows the contour map of reflectance variation of AMSs as a function of height (0–5 μm) and wavelength (1–5 μm) for a period of (a) 1 μm and (b) 5 μm. As expected, the flat surface (height = 0 μm) of ZnS substrate exhibits the reflectance of ~15 % for single surface. As the height increases, the reflectance tends to decrease. This can be explained by the fact that the effective refractive index is gradually changed. At the height of 5 μm, the AMSs with parabola shape provide an average reflectance of less than 1.0 % in both cases. In case of 1 μm period, very low reflectance can be obtained in whole mid-IR ranges while the AMSs with 5 μm period have higher order diffraction losses at shorter wavelength ranges. The parabola shaped AMSs with 1 μm period can be fabricated by laser interference lithography, thermal reflow, and subsequent pattern transfer process (Song et al. 2010). The thermal reflow of photoresist patterns enlarges the packing density as well as convert the geometry from rod to lens, which enables closely packed parabola structures. If the AMSs need few-micron periods, conventional photolithography can be applied.

Figure 3 shows the influence of the height of the array on the reflectance as a function of the period and wavelength (1–15 μm). When the grating period is near one micron, the height of 1 μm is reasonable to cover whole mid-IR ranges, as depicted in Fig. 3a. If the height increases from 1 to 3 μm, the AR band is extended to far-IR ranges (>12 μm), as depicted in Fig. 3b. Because the aspect-ratio of 1–5 is acceptable in the dry etch process, we can choose the period and height from this contour plot by considering the target applications/spectra. In this case, the optical bandwidth is in the range of 1–5 and 8–14 μm, which covers whole atmospheric transmission bands (Loubere 2012). This bandwidth can be tuned by changing the periods and heights. The white dashed lines in Fig. 3a, b indicate the border lines between the diffraction orders. Even though the structure with period of 3 μm and height of 3 μm exhibits low reflection, it generates higher order transmission (Fig. 3c), while the structure with period of 1 μm provide only zeroth order diffraction (Fig. 3d).

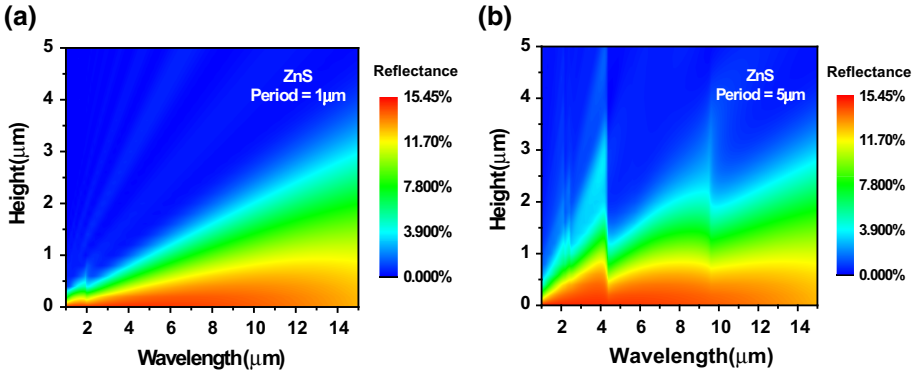

Fig. 2 Contour plot of the variation of reflectance of AMSs with a period of **a** 1 μm and **b** 5 μm, respectively, as a function of height and wavelength

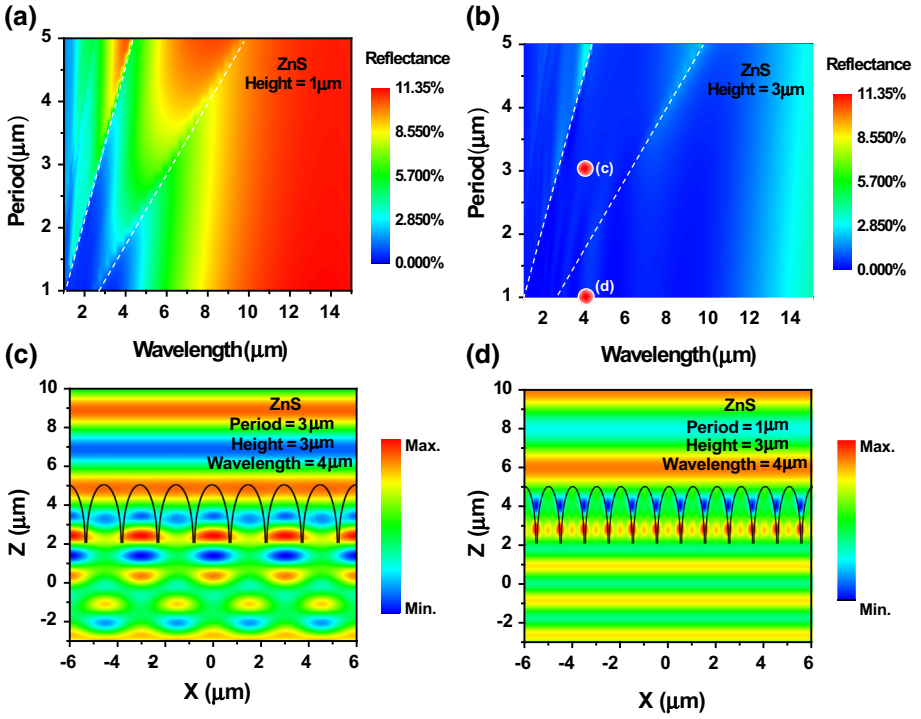

Fig. 3 **a**, **b** Contour plot of the variation of reflectance of AMSs with a height of **a** 1 μm and **b** 3 μm, respectively, as a function of period and wavelength. **c**, **d** Electrical field intensity distributions of AMSs with height of 3 μm and period of **c** 3 μm and **d** 1 μm, respectively, at 4 μm incident wavelength

Other IR materials, such as Ge, ZnSe, and silicon (Si), are also commonly used for imaging devices or photodetectors in the mid- and/or far-IR ranges. Since the diffraction efficiency of grating structures is strongly dependent on the refractive index of media, it is worthwhile to investigate the reflection maps for different IR materials. As indicated in Fig. 4a, the refractive indices of four different materials are nearly flat in IR spectral ranges. Figure 4b–d shows a straightforward tendency between the gradient of border line and the refractive index. Because the Ge has higher index compared to that of other materials, higher order diffraction occurs at shorter period. In other words, tolerance in period of the higher index material is narrow than that of lower index material.

The geometry of AMSs is crucial to determine the diffraction efficiency. It is well known that the parabola shape has superior AR properties in a broader wavelength range due to their linearly graded index profile. In some case, however, precise fabrication procedure is needed to generate ideal shape. Figure 5 shows the effect of AMSs' geometry on the reflection characteristics. The shape of AMS is changed from cylindrical rod to paraboloid with 20 steps, as depicted in Fig. 5. The cylindrical rods have ripple patterns on the reflectance curve, because the pattern acts as a single layer antireflection coating. As the shape of AMS goes to tapered shape, the reflectance fluctuation is released and it shows broadband AR properties. It is noted that the AR performance of AMSs with parabolic ratio of $\sim$80 % provides comparable to that of ideal paraboloid.

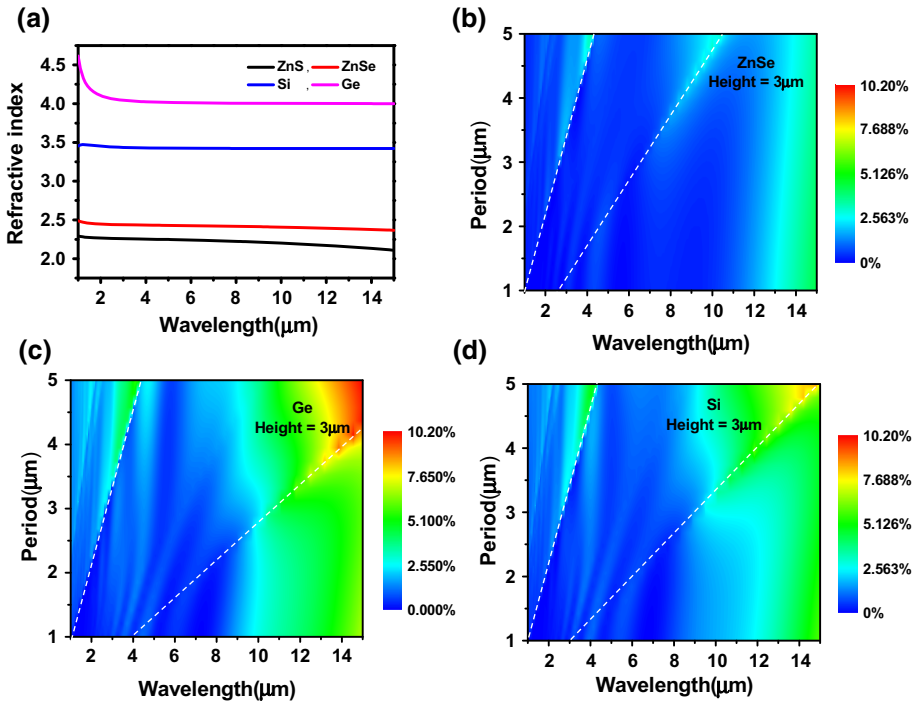

Fig. 4 **a** Refractive index curves of four different semiconductor materials (i.e., ZnS, ZnSe, Si, and Ge) in the wavelength range of 1 to 15 μm. **b**, **d** Contour maps of reflectance for **b** ZnSe, **c** Ge, and **d** Si, respectively, versus period and wavelength

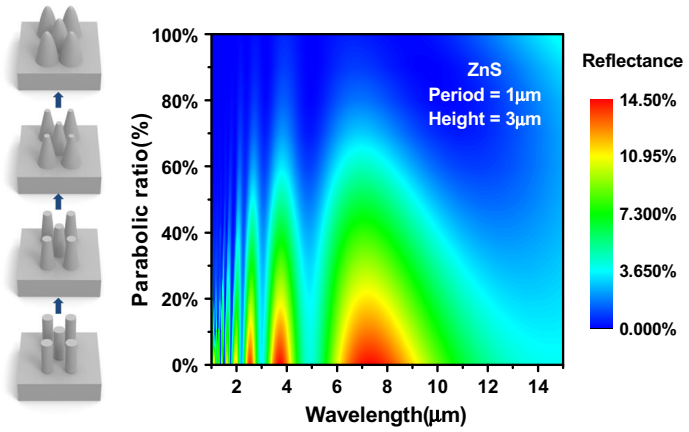

Fig. 5 Contour plot of the variation of reflectance of AMSs with different shapes. The shape is changed from cylindrical rod (*bottom*) to paraboloid (*top*), continuously. The period and height was fixed to 1 and 3 μm, respectively

3 Conclusion

By considering the fabrication procedure and tolerance, we investigated optimum geometry of ZnS AMSs with parabola shape for mid- and far-IR applications. From the contour plots, the effects of the heights and periods on the reflectance were also analyzed. The ZnS AMSs with optimized geometry can be used to applications including night vision, thermal imaging, motion sensors, astronomy, and forward looking infrared (FLIR) technology (Rowan 2013; Miller 1994). Furthermore, it can be extended for other applications such as photovoltaics (Li et al. 2014) and electromagnetic wave sensing (Zhang et al. 2014) by using different materials and changing the periods and heights.

Acknowledgments Y. J. Yoo and K. S. Chang contributed to this work equally. This work was partly supported by the Korea Basic Science Institute grant (D34500), by Basic Science Research Program through the National Research Foundation of Korea (NRF) funded by the Ministry of Science, ICT & Future Planning (2014R1A1A1005945), and by BK21PLUS, Creative Human Resource Development Program for IT Convergence.

References

Ghosh, A., Bandyopadhyay, P.K.: Broad band antireflection coating on silicon from 1.5 to 6 μm spectral band. Infrared Phys. Technol. **46**, 408–411 (2005)

Kanamori, Y., Sasaki, M., Hane, K.: Broadband antireflection gratings fabricated upon silicon substrate. Opt. Lett. **24**, 1422–1424 (1999)

Lalanne, P., Morris, G.M.: Design, fabrication and characterization of subwavelength periodic structures for semiconductor anti-reflection coating in the visible domain. Proc. SPIE **2776**, 300–309 (1996)

Li, X., Dasika, V.D., Li, P.-C., Ji, L., Bank, S.R., Yu, E.T.: Minimized open-circuit voltage reduction in GaAs/InGaAs quantum well solar cells with bandgap-engineered graded quantum well depths. Appl. Phys. Lett. **105**(12), 123906 (2014)

Loubere, P.: The global climate system. Nat. Educ. Knowl. **3**, 24 (2012)

Miller, J.: Principles of Infrared Technology. Springer, Berlin, 978-1-4615-7666-2 (1994)

Moharam, M.G.: Coupled-wave analysis of two-dimensional dielectric gratings. Proc. SPIE **883**, 8–11 (1988)

Phillips, R.R., Haynes, V., Naylor, D.A., Ade, P.: Simple method for antireflection coating ZnSe in the 20 μm wavelength range. Appl. Opt. **47**, 870–873 (2008)

Rogalski, A., Chrzanowski, K.: Infrared devices and techniques. Opto-Electron. Rev. **10**, 111–136 (2002)

Rowan, M.: Night Vision: Exploring the Infrared Universe. Cambridge University Press, Cambridge 978-107-02476-2 (2013)

Song, Y.M., Jang, S.J., Yu, J.S., Lee, Y.T.: Bioinspired parabola subwavelength structures for improved broadband antireflection. Small **6**, 984–987 (2010)

Song, Y.M., Park, G.C., Jang, S.J., Ha, J.H., Yu, J.S., Lee, Y.T.: Multifunctional light escaping architecture inspired by compound eye surface structures: from understanding to experimental demonstration. Opt. Express **19**, A157–A165 (2011)

Striemer, C.C., Fauchet, P.M.: Dynamic etching of silicon for broadband antireflection applications. Appl. Phys. Lett. **81**, 2980–2982 (2002)

Yu, Z., Gao, H., Wu, W., Ge, H., Chou, S.T.: Fabrication of large area subwavelength antireflection structures on Si using trilayer resist nanoimprint lithography and liftoff. J. Vac. Sci. Technol., B **21**, 2874–2877 (2003)

Zhang, X., Hosseini, A., Subbaraman, H., Wang, S., Zhan, Q., Luo, J., Jen, A.K.-Y., Chen, R.T.: Integrated photonic electromagnetic field sensor based on broadband bowtie antenna coupled silicon organic hybrid modulator. J. Lightwave Technol. **32**(20), 3774–3784 (2014)